D.B.Hondongwa and E. R. Fossum, "Temporally oversampled CMOS X-ray photon-counting sensor for low-dose fluoroscopy," 2017 IEEE 60th International Midwest Symposium on Circuits and Systems (MWSCAS), Boston, MA, 2017, pp. 1101-1104.

Temporally Oversampled CMOS X-ray Photon Counting Sensor for Low Dose Fluoroscopy

Donald B. Hondongwa and Eric R. Fossum
Thayer School of Engineering
Dartmouth College
Hanover, NH, USA

***Abstract*—We present an x-ray quanta image sensor (XQIS) utilizing temporal oversampling and CMOS image sensor technology. The output of the XQIS is a binary bit frame with each bit representing the presence or absence of a detected x-ray photon. The bit frames are read out at very high rate (>1000fps) and a series or bit values are combined to form pixel values using digital frame integration. A system model analyzing the design parameter is presented and the component designs are evaluated in simulation.**

Keywords*— *CMOS image sensors, photon counting, high-speed sensor, x-ray imaging

I. INTRODUCTION

X-ray imaging is one of the main pillars of medical imaging allowing for non-invasively viewing the internal structure and functioning of organisms [1, 2]. The penetrating power of x-rays makes them invaluable for such applications. Innovation in the field is driven by the need for lower dose per image to reduce patient exposure to the ionizing radiation. Current research to this end is focused on x-ray photon counting [3].

Image sensors can be categorized according to how they account for the x-ray photons with the 2 main categories being the current integrating detectors (CID) and the photon counting detectors (PCD). The pixel value in CIDs is proportional to the time integral of the photoelectric current generated as a result of photon absorption in the sensor. In contrast, PCDs produce a pixel value that is proportional to the photon count incident on the detector. In x-ray imaging, photon counting aims to quantify the number of x-ray quanta received by the sensor. One of the advantages of PCDs is that while CID images are weighted more toward the high-energy end of the x-ray spectrum, which unfortunately contains less diagnostically relevant information, photon counting can provide equal weighting to the photons [3]. If energy discrimination is implemented in the detector, the energy weighting can be optimized. Resultantly, PCDs have been shown to have better dose efficiency meaning they make better use of the available information in the x-rays [4].

Several approaches have been proposed to implement photon counting in x-ray imaging [5-7]. These counting schemes are typically based on direct detection and continuous time current monitoring schemes. The absorption of an x-ray photon creates a current pulse in the detector. The current pulse is processed using pulse shaping circuitry, thresholding comparators, and counters. Energy resolved imaging has also been implemented using multiple thresholds to determine the size of the current pulse, a value that relates the absorbed x-ray photon energy [3]. The disadvantage with these systems is that they require continuous current monitoring which means that each pixel must contain all this circuitry. Additionally, the use of exotic direct detector material can increase the cost of the devices.

We propose using an indirect imaging approach with temporal oversampling to perform photon counting using 4T pixel based CMOS detectors with column-parallel signal processing for low dose fluoroscopy. The use of column parallel processing circuitry, as opposed to pixel level processing, removes the area limitations on the processing circuitry as well as improving uniformity due to the shared circuitry. The temporal oversampling can be used for motion detection and correction in real time imaging modes like fluoroscopy.

A prototype sensor was designed and fabricated in a 0.18μm CMOS image process with 100μm pixels utilizing the 4T active pixel topology. The paper presents a discussion of the system concept, a model for parameter optimization and design of the prototype.

II. DEVICE CONCEPT

The system uses an indirect x-ray imaging approach in which a scintillator absorbs the incoming x-ray photons and converts them into lower energy optical photons. Thallium-activated cesium iodide (CsI:Tl) and gadolinium oxysulfide (Gd_2O_2S) are good candidates due to the high scintillator gain and relatively fast response. Additionally, the emission spectrum for these scintillators is centered at 550 nm and 510 nm respectively [8], which matches well with the absorption spectrum of silicon. The scintillator is optically coupled to a CMOS image sensor allowing the generated optical photons to be detected. The optical coupling can be done by placing the scintillator directly on the array, or through a fiber optic plate. Fig. 1 shows the indirect imaging approach with the scintillator optically coupled to the sensor with a fiber optic plate.

This work has been supported by Varex Imaging Corporation and Varian Medical Systems.

978-1-5090-6389-5/17/$31.00 ©2017 IEEE

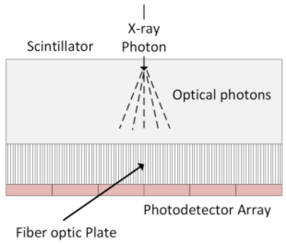

Fig. 1. An illustration of indirect x-ray imaging. The scintillator is optically couple to the photodiode with a fibre optic plate.

With temporal oversampling, there is a corresponding reduction in the photon flux per pixel and by imaging at speed in excess of 1000 fps, the probability of multiple x-ray photons being incident on any one pixel in an imaging frame is small. Resultantly, the integrated photons can be taken to be from one x-ray photon event. The integrated signal in the pixels is converted to a voltage using a capacitive sense node. A column parallel thresholding system is used to determine the occurrence of an x-ray event. The result of each integration frame is a bit plane corresponding to the photon event similar to the bit planes in quanta image sensing [9]. Digital integration is used to combine the bit plane to form an image. The simplest method will be adding up the bits. More complex processing is possible to correct for motion artifacts.

III. System Model

The performance of the system will depend on several design parameters and operating conditions. To evaluate the effect of the parameters, the system is analyzed using a cascaded signal transfer model. In this type of a model, the impact of each stage on the signal is studied to develop a model of how the system would perform [10].

The goal of the system is to count the incident x-ray quanta, but as an imperfect system, there will be errors. The bit error rate is a metric typically used to quantify the counting errors in photon counting systems [11]. Several scenarios can result in counting errors:

1) *Multiple x-ray quanta in a frame*

   The random nature of x-ray photon arrival means that there is a non-zero probability of the multiple events in the same bit frame. The events can only be recorded as 1 resulting in error.

2) *Charge sharing*

   The charge cloud generated by a single x-ray event can spread to neighboring pixels resulting in erroneous counts.

3) *Missed counts*

   This is the case when an x-ray event occurs but fails to trigger a recorded event in the sensor.

4) *Ghost counts*

   Ghost counts are when a pixel registers a count in the absence of a corresponding x-ray event.

A time sensitive stochastic computer model was used to simulate the effect of the design parameters on the performance. The simulation that keeps track of the signal from each x-ray at each stage of the imaging system and the error rates are determined from an ensemble of the responses.

A. X-ray Photon Arrival - Photon Statistics

The photon arrival at a detector surface follows the Poisson distribution. Given an average absorbed photon flux φ, the probability of k photon arrivals a time window of width τ is given by (1).

$$P[k] = \frac{e^{-(\varphi\tau)}(\varphi\tau)^k}{k!} \tag{1}$$

From this equation, we can determine that the probability of one or fewer photon arrivals in a time window is described by (2), the exposure H is given by $H = \varphi\tau$.

$$P[k \leq 1] = e^{-H}(1 + H) \tag{2}$$

Equation (2) show that reduction of the exposure improves the accuracy of the detector; reducing H from 1 to 0.5 reduces the probability of multiple counts by over 65%.

B. Signal generation

The absorption of x-ray photons in the scintillator can be modeled as a gain stage. The number of optical photons created is dependent on the energy and the gain of the scintillator. As the generated photons traverse the scintillator, they interact with the scintillator material scattering and getting absorbed along the way. A portion of the generated photons exits the scintillator in the direction of the detector. Equation (3) describes the average number of optical photons, $\overline{q_{op}}$ incident of the photodetector where E is the energy of the x-ray photon, $\bar{g}$ is the average gain of the scintillator and η is the escape probability.

$$\overline{q_{op}} = \bar{g}E\eta \tag{3}$$

The spatial distribution of the optical quanta can be approximated by a Gaussian distribution [10, 12] and the time distribution can be approximated with an exponential decay whose decay constant is a material property of the scintillator [8].

C. Signal detection

Equation (4) describes the pixel output voltage (S) as the integrated optical photoelectrons multiplied by the conversion gain (CG) plus the additive read noise (n). Signal thresholding is then performed to determine if an x-ray absorption event likely occurred and a counter is used to keep track of the photon counts.

$$S = CG \cdot \int_{t_0}^{t_0+\tau} \int_{y_{min}}^{ymax} \int_{x_{min}}^{x_{max}} q(x, y, t)\, dx \cdot dy \cdot dt + n \tag{4}$$

The model was implemented Matlab. X-ray events were generated with event times calculated from Poisson distributed wait times and randomly distributed locations. For each event, secondary photons are generated with the location being sampled from a Gaussian distribution centered on the location of the x-ray event and times randomly picked from the exponential curve. The signal in each pixel is integrated, and a random read noise value is added. The resulting value is then compared to a threshold. Error rates are calculated by comparing the incident x-ray counts and the resulting counts. The probability of multiple counts is the fraction of frames with more than one simulated x-ray event and the probability of charge sharing is the fraction of frames that registered events in more than one pixel. The ghost and missed counts metric were measured as the number of frames with counts were register but no corresponding event occurred and vice versa.

IV. Modeling Results and Discussion

The developed Matlab model was used to investigate the effect of several design parameters. Fig. 2 shows the effect of the exposure on the error rate. As the exposure increases, the probability of multiple x-ray events per pixel per frame increases. An interesting feature of this curve is that the sensor does not have a hard saturation at exposures greater than one, but instead shows an over exposure latitude similar to that of film [9]. This means that even for larger flux rate, the sensor is still useful. The charge sharing error is also shown in Fig. 2. With higher exposure, charge sharing also increases. This is a result of the increased likelihood that events are closer to the pixel border resulting in charge sharing.

The results in Fig. 2 show the error rate as a function of the threshold level normalized to the signal level. Low threshold relative to the signal increases the probability of charge sharing errors because even a small amount of signal in the neighboring pixel well trigger an event. On the other hand, a high threshold result is an increase in missed counts. An optimal threshold is thus closer to half the signal level.

The effect of the noise on the counting accuracy is shown in Fig. 2. For low noise levels, the counts are relatively immune to the noise. For higher noise level, the rate of both ghost counts and missing counts increases as the signal gets distorted by the noise. The effect of pixel length on the system is shown in Fig. 2. Changing the pixel pitch effectively changes the number of photon per pixel, hence it has a similar effect changing the photon flux. One significant difference is that the rate of missed counts increases for small diodes. This is because the charge is being spread over more pixels resulting in an insufficient signal to trigger the comparator in any of the pixels.

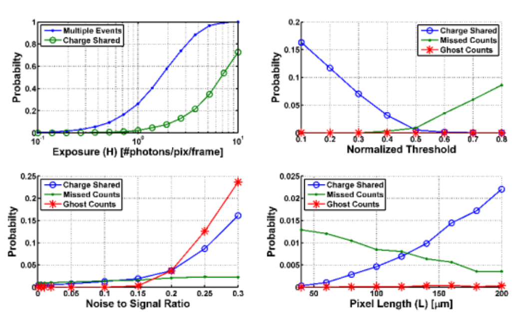

Fig. 2. The results of model simulations showing the error rate in response to exposure (top left), threshold voltage (top right), noise (bottom left), pixel length (bottom right)

Table 1: Summary of prototype specifications

Specification	Value
Technology	X-Fab 0.18µm CIS process
Supply	3.3V
Pixel	4T active pixel
Pixel pitch	100 µm
Fill factor	>80%
Sensor speed	1000 fps
ADC	3 bit flash

V. Prototype Design

A prototype was designed to implement the proposed imaging concept. A summary of the design specifications is shown in Table 1 and Fig. 3 shows a high-level schematic of the system.

The sensor uses 4T active pixels for photon detection. A schematic of the 4T pixel is shown in Fig. 3. The optical photons are absorbed in the photodiode (PPD) to create photoelectrons. After the integration time the collected photoelectrons are transferred to the FD capacitor through the transfer gate (TG). Immediately before the transfer, the FD voltage is reset using the reset switch (RST). The reset level is read on the column line via the source follower (SF) and the row select switch determines which row currently drives the column line. After the charge transfer, the pixel output is read out again, and correlated double sampling (CDS) is performed

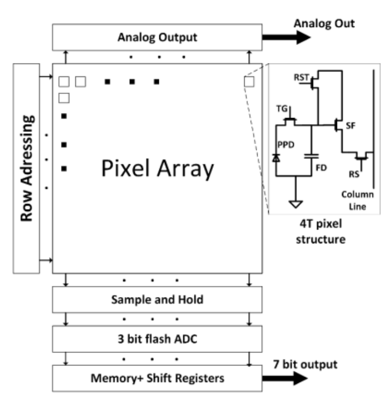

Fig. 3. System schematic showing the pixel array and the processing circuitry. The figure also show the schematic of the 4T pixel

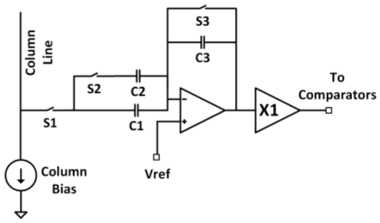

Fig. 5. Schematic of the column amplifier

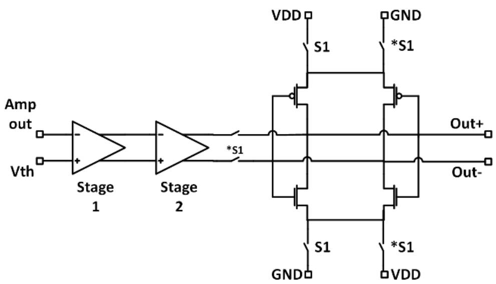

Fig. 6. Schematic of the comparator using a cascaded multi-stage pre-amplifier

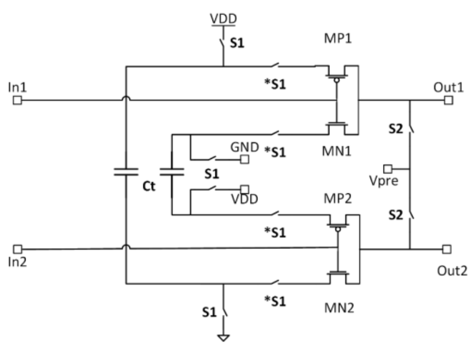

Fig. 7. Schematic of the differential charge transfer amplifier in a single stage of the comparator

to determine the amount of integrated charge. A column parallel switched capacitor programmable gain amplifier is used to perform correlated double sampling. Fig. 5 shows a schematic of the column amplifier.

Comparators compare the output of the amplifier to preset thresholds. Each column has 7 comparators. The comparators consist of a 2-stage pre-amplifier and a latch. Fig. 6 shows the schematic of the comparator. Each stage of the pre-amplifier is a differential charge transfer amplifier. This topology can provide amplification high gain while consuming low power [13]. A schematic of the CTA is shown in Fig. 7.

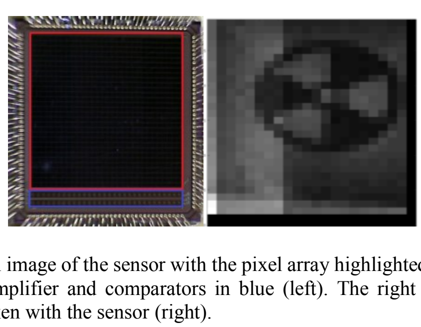

Fig. 4. An image of the sensor with the pixel array highlighted in red and column amplifier and comparators in blue (left). The right image is a picture taken with the sensor (right).

The prototype designs were fabricated and packaged. The chip is functional and detailed testing is currently underway. Fig. 4 shows an image of the chip highlighting the pixel array and the processing circuitry. Also included in Fig. 4 is an optical image captured by the sensor during preliminary testing.

VI. Conclusion

A time sensitive model and implementation of temporal oversampled CMOS image sensor based XQIS system has been presented. The model provided a means of comparatively evaluating the performance of the detector with respect to the design parameter space. Future extension of the work will include expanding the model to simulate the interactions with matter. The Effect of fill factor and charge transfer specifics will be included.

Acknowledgment

The authors thank X-Fab for support in building test devices and Varex Imaging Cooperation for the financial and technical support.

References

[1] B. Kevles, "Naked to the bone: Medical imaging in the twentieth century,", 1997.
[2] J.T. Bushberg, "The essential physics of medical imaging,", 2012.
[3] K. Taguchi and J.S. Iwanczyk, "Vision 20/20: Single photon counting x-ray detectors in medical imaging," Med.Phys., vol. 40, no. 10, 2013, pp. 100901.
[4] M. Danielsson, H. Bornefalk, B. Cederstroem, et al, "Dose-efficient system for digital mammography,", vol. 3977, 2000, pp. 239-249.
[5] M. Campbell, E. H. M. Heijne, G. Meddeler, E. Pemigotti and W. Snoeys, "Readout for a 64x64 pixel matrix with 15-bit single photon counting," 1997 IEEE Nuclear Science Symposium Conference Record, 1997, pp. 189-191 vol.1.
[6] R. Ballabriga, M. Campbell, E. H. M. Heijne, X. Llopart and L. Tlustos, "The Medipix3 Prototype, a Pixel Readout Chip Working in Single Photon Counting Mode with Improved Spectrometric Performance," 2006 IEEE Nuclear Science Symposium Conference Record, vol. 6, 2006, pp. 3557-3561.
[7] W.C. Barber, E. Nygard, J.S. Iwanczyk, et al, "Characterization of a novel photon counting detector for clinical CT: count rate, energy resolution, and noise performance,", vol. 7258, 2009, pp. 725824.
[8] C. Greskovich and S. Duclos, "Ceramic scintillators,", vol. 27, no. 1, 1997, pp. 69-88.
[9] Jiaju Ma, D. Hondongwa and E. R. Fossum, "Jot devices and the Quanta Image Sensor," 2014 IEEE International Electron Devices Meeting, 2014, pp. 10.1.1-10.1.4.
[10] J. Xu, W. Zbijewski, G. Gang, et al, "Cascaded systems analysis of photon counting detectors," Med.Phys., vol. 41, no. 10, 2014, pp. 101907.
[11] E. R. Fossum, "Modeling the Performance of Single-Bit and Multi-Bit Quanta Image Sensors," IEEE Journal of the Electron Devices Society, vol. 1, no. 9, 2013, pp. 166-174.
[12] M. Freed, S. Park and A. Badano, "A fast, angle-dependent, analytical model of CsI detector response for optimization of 3D x-ray breast imaging systems," Med.Phys., vol. 37, no. 6, 2010, pp. 2593-2605.
[13] S. Masoodian, K. Odame and E. R. Fossum, "Low-power readout circuit for quanta image sensors," Electronics Letters, vol. 50, no. 8, 2014, pp. 589-591.